Available online at www.sciencedirect.com
SCIENCE DIRECT®
Optik 116 (2005) 265–269
Optik Optics
www.elsevier.de/ijleo

LCD pixel shape and far-field diffraction patterns

M. Fernández Guasti[a,*], A. Meléndez Cobarrubias[b], F.J. Renero Carrillo[b], A. Cornejo Rodríguez[b]

[a]*Laboratorio de Óptica Cuántica, Universidad Autónoma Metropolitana - Unidad Iztapalapa, Ap.Postal 55-534, México 09340 D.F., México*
[b]*Instituto Nacional de Astrofísica, Óptica y Electrónica, Coordinación de Óptica, Apdo. Postal 51 y 216, 72000 Puebla, Pue., México*

Received 8 November 2004; accepted 29 January 2005

Abstract

The shape and diffraction pattern of a liquid crystal display (LCD) pixel used in a point-diffraction interferometer is qualitatively evaluated using the experimental diffraction patterns of computer-generated apertures. The diffraction patterns for apertures with contours between a circle and a square were numerically plotted from analytical expressions of these topological forms. The observed patterns are qualitatively in accordance with previous calculations of such apertures using scalar diffraction theory in the far field.

Keywords: Point diffraction interferometer (PDI); LCD; squircle

1. Introduction

Liquid crystal displays (LCD) are now being extensively used in many devices. Large arrays are employed in TV screens and computer displays whereas high-resolution small arrays are used in digital projectors and interferometric devices. Pixels in LCDs are usually described by squares but in practice their shape resemble a square with blunt corners as we shall presently exhibit.

The Fraunhofer diffraction patterns of circular, square or rectangular apertures are well known since the early development of scalar diffraction theory. However, squares with blunt corners or intermediate figures between a circle and a square have only been recently theoretically tackled using the scalar theory in the far-field limit [1]. The Fourier Bessel integrals that are obtained for these apertures may be integrated analytically on the radial variable whereas the angular integral has to be evaluated numerically.

Point-diffraction interferometers (PDI) rely on the interference of the wave front under test with a reference wave front that arises from a pinhole whose diffraction pattern is assumed to be a perfect spherical wave front [2,3]. Recent versions of the PDI use a LCD with all pixels dark but one in order to produce the pinhole mask [4,5]. In these type of applications, it is particularly important to characterize the diffraction pattern of the aperture since it is used as the reference measuring wave front.

In this communication, the diffraction pattern of LCD pixels are compared with the diffraction patterns produced by numerically generated apertures. In Section 2, the equation governing the outline of the apertures is discussed. The photographic masks produced with these forms and the arrangement used to

*Corresponding author.
E-mail address: mfg@xanum.uam.mx (M. Fernández Guasti).

0030-4026/$ - see front matter © 2005 Elsevier GmbH. All rights reserved.
doi:10.1016/j.ijleo.2005.01.018

record the diffraction patterns are also described in this section. In Section 3, the experimental layout of one or more pixels produced by a LCD mask is presented. In Section 4, the experimental results are exposed and their main features discussed. The shape of the LCD pixel is inferred from its diffraction pattern through comparison with the computer-generated apertures. The LCD aperture used in a PDI, rather than the ideal circular symmetry, has the shape of a square with blunt corners. The conclusions are drawn in Section 5.

2. Photographic masks

Intermediate figures between a circle and a square may be described analytically through a single equation restricted to the appropriate domain [6]. The apertures produced with this algorithm yield figures that resemble squares with blunt corners. These silhouettes may be adequate for modeling the shape of pixels produced by diverse digital imaging systems. This assertion will, in fact, be supported by the results presented hereafter. The photographic diffracting apertures employed in this work were generated from the *squircle* equation, that is, the equation for a square/circular aperture. The polar equation for a *squircle* form is given by

$$\frac{s^2}{4}\sin^2(2\theta)r^4 - k^2r^2 + k^4 = 0, \tag{1}$$

where (r,θ) are the polar coordinates at the aperture plane and "s" is the squareness parameter [6]; $s=1$ represents a square with sides equal to $2k$, while $s=0$ represents a circle of radius k. The equation for the square is perhaps more clearly visualized in Cartesian coordinates with the substitution $4x^2y^2 = r^4\sin^2(2\theta)$. The Cartesian equation for a *squircle* is

$$s^2\frac{x^2}{k^2}\frac{y^2}{k^2} - \left(\frac{x^2}{k^2}+\frac{y^2}{k^2}\right) + 1 = 0. \tag{2}$$

This expression may be factored for $s=1$ into $(1-x^2/k^2)(1-y^2/k^2)=0$, which yields a square when the restriction $x^2, y^2 \leqslant k^2$ is imposed. The parameter "s" is a good measure of how sharp or blunt are the corners of the square. This parameter may be continuously varied to smoothly change the shape of the contour from a circle to a square. The change in the aperture shape is more sensitive when "s" is close to one. A typical computer-generated aperture plot for $s=0.9$ is shown in Fig. 1. The area lying outside the curve was rendered in black in order to produce the aperture mask. The plots of the squircle equation for various squareness values were recorded in high-contrast photographic film reducing their size to about 1 mm in diameter, that is $k=0.5$ mm. The upper left-hand quadrant of the diffracting apertures was photographed with an optical microscope in order to monitor the actual shape of the apertures.

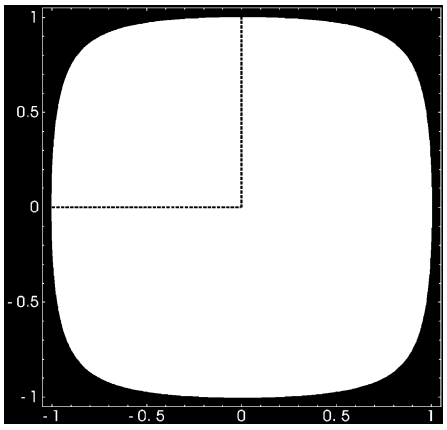

Fig. 1. Diffracting aperture plot for squareness parameter $s=0.9$.

The form of the aperture in the other three quadrants is symmetrical with respect to the quadrant shown in the microphotographs.

The apertures were illuminated directly with a HeNe laser placed 2 m apart from the aperture plane. The diffraction patterns were recorded on high-resolution color film located 3 m apart from the diffracting apertures. This distance was appropriate in order to consider the pattern to be in the far field and also to fill reasonably well the 35 mm film that was used to photograph these patterns. This simple arrangement was favored in order to avoid contributions from intermediate optical elements.

3. Experimental setup

The experimental setup used to obtain the images and diffraction patterns of the LCD pixels is shown in Fig. 2. The display is a monochrome active matrix twisted nematic crystal consisting of an array of 320×240 pixels with maximum contrast ratio of 80 to 1 (Kopin, CyberDisplay 320). The pixel dimensions given in the specifications is $15\,\mu m \times 15\,\mu m$ and the separation between pixels is 25 μm. This display was controlled with a personal computer. The screen resolution was adjusted so that individual pixels could be turned on (full transparency) or off (fully darkened). The display was mounted on an xyz mount and placed in the vicinity of the beam waist where it is commonly positioned in a PDI scheme.

Images of the open pixels were taken using a traveling microscope and white light illumination. These images were used to confirm the position and the number of active pixels. The diffraction patterns of the pixels were taken under HeNe laser illumination. The laser beam was spatially filtered and collimated following the usual layout of a PDI. The image was detected with a CCD

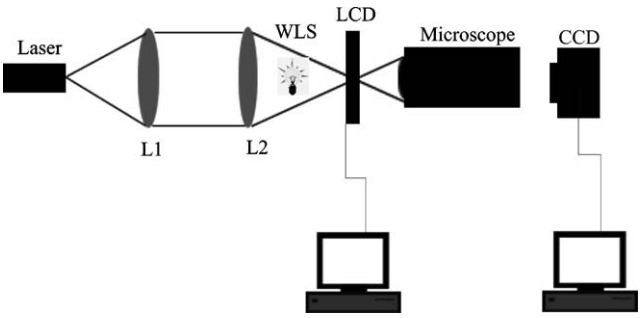

Fig. 2. Experimental setup. LCD is the liquid crystal display diffracting aperture. The diffraction pattern is observed via a charged-coupled device (CCD). The microscope and the white light source (WLS) are used in order to observe the pixels directly but are removed when the diffraction pattern is recorded.

placed instead of the microscope 50 cm after the LCD plane. A second computer was used to acquire the CCD image.

4. Results

The computer-generated aperture shapes together with their corresponding diffraction patterns are shown in Figs. 3a–e. The microscope photographs of the apertures reveal that their shape is not as smooth as the original plots. This raggedness is likely to be due to the grain of the photographic film. The larger the size of the apertures the smaller is the relative effect of the film grain; however, the diffraction patterns become correspondingly smaller and a compromise has to be established.

The diffraction patterns were photographed using different exposure times. Short times reveal the intensity distribution of the central lobe but higher orders are not detected whereas longer times saturate the central lobe while higher orders are recorded. Diffraction patterns are usually difficult to photograph due to the large range of intensities that need to be recorded. A compromise is required in order to observe the desired features in the region where the film exhibits a linear response. Digitizing the images is not of great help since it is difficult to maintain linear relationships between the neutral density of the film and the incident intensity.

The sequence in Figs. 3a–e shows how the initial Sinc(x)Sinc(y) diffraction pattern of a square is modified in various steps of the squareness parameter. The second-order maxima in each figure illustrate most clearly the evolution of the sequence. The four lobes around the central maximum obtained for the square aperture, merge into one another in the subsequent figures until one has a squarish ring with uneven but finite intensity for all angles as may be seen in Fig. 3c.

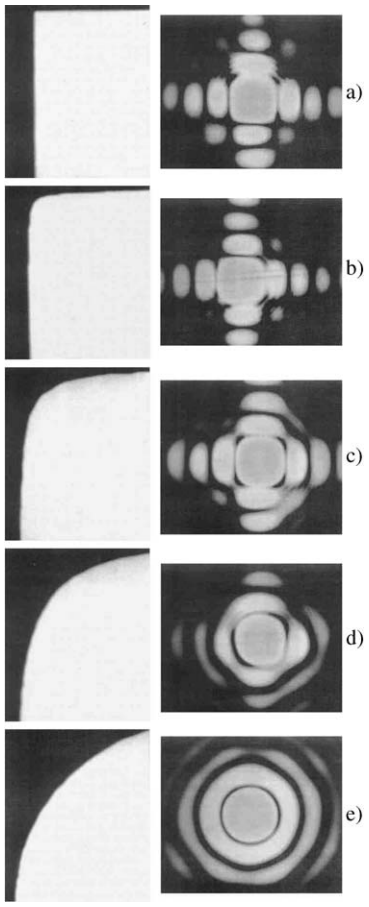

Fig. 3. (a) $s = 1.0$ – on the left a microphotograph of the upper left-hand corner of the aperture is shown. The right-hand side shows a photograph of the far-field diffraction pattern produced by the aperture; (b) $s = 0.995$ – a small departure of the squareness parameter already reveals an appreciable roundness of the corner of the square; (c) $s = 0.9$ – the secondary maxima in the diffraction pattern begin to spread out and commence to "touch" each other; (d) $s = 0.8$ – the secondary maximum is clearly a ring although it still exhibits lobes reminiscent of the square aperture and (e) $s = 0.001$ – the Airy pattern corresponding to a circle is obtained. The secondary maximum is a ring with circular symmetry.

The shape of the rings come closer to a circular contour as the aperture approaches the circular form. Simultaneously, the intensity distribution as a function of angle becomes more smooth. Airy rings are obtained in Fig. 3e that correspond to the diffraction pattern of a circle. These features are in qualitative accordance with the numerical estimates obtained from the Fourier Bessel integrals [1]. Fig. 4 shows a representative contour plot and mesh that evaluate the Fourier Bessel transform of the wave amplitude in the far-field limit.

It should be noted that higher-order rings show an unequal intensity as a function of the angle even for the circular aperture. This irregular behavior is presumably due to the raggedness of the aperture. Higher spatial

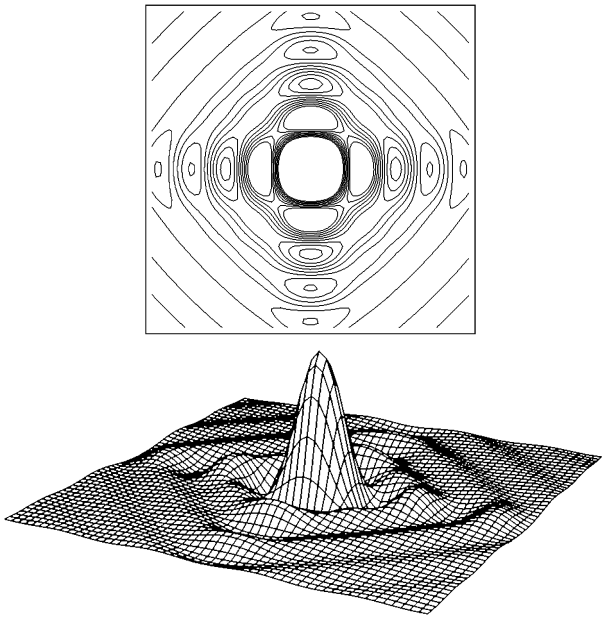

Fig. 4. Diffraction pattern of squircle with $s = 0.9$; contour plot for iso-amplitudes shown on the top and 3D mesh with height representing the field amplitude on the bottom.

frequencies on the aperture have stronger influence on higher-order rings or further away from the axis in the diffraction pattern [7].

Let us now exhibit the images and diffraction patterns obtained with the LCD mask. The microscope image of a single LCD pixel together with its far-field diffraction pattern is shown in Fig. 5. The low resolution of the traveling microscope yields an image whose squarish shape may only be approximately guessed from the photograph. However, comparison of the diffraction pattern of the pixel with the previous patterns shows that the pixel is not a perfect square with sharp corners. The most similar diffraction image is 3c, which indicates that the pixel has blunt corners with a squareness parameter around $s = 0.9$. The reference wavefront in a PDI will have this pattern when implemented with an LCD pixel of this type. Departure from the point source circular symmetry is expected even if only the central portion is considered as may be seen from the contour plot in Fig. 4. This discrepancy with the spherical wavefront should then be taken into account so that it is not associated, for example, with aberrations of an optical system under test.

In Fig. 6, the image and diffraction pattern of an array of nine apertures are shown. The contribution of the square pixels blunt corners is still clear in the diffraction pattern. On the one hand, full rings rather than the spots expected from the square array are clearly visible. On the other hand, the rings are not circular but are flattened at 45° from the Cartesian axes. Furthermore, the rings are more intense in the regions where perfect squares would exhibit their maxima. The diffraction pattern, according to Fourier optics theory, should correspond to the convolution of the single pixel aperture that is shifted to the other eight positions in the aperture plane.

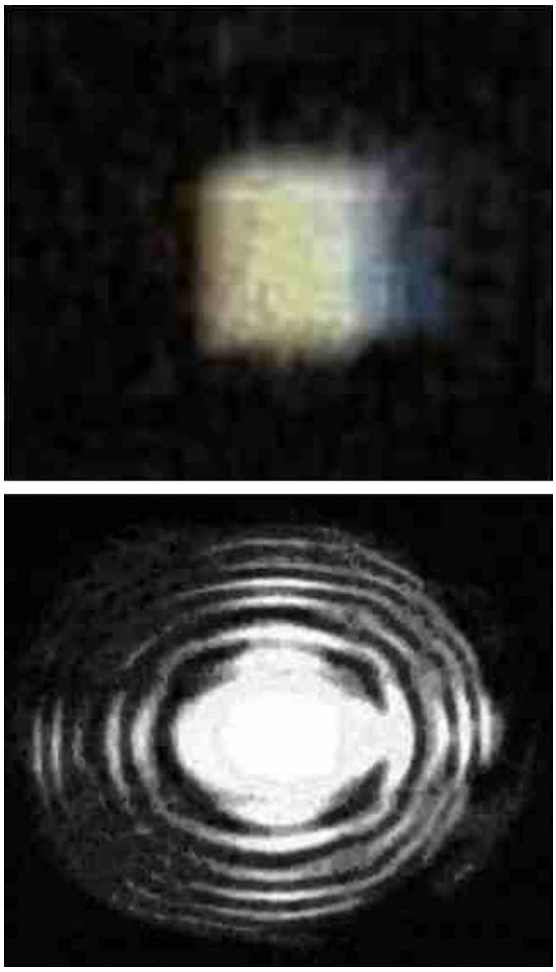

Fig. 5. Image of a single LCD pixel (top) and the corresponding diffraction pattern in the far field (bottom).

5. Conclusions

The far-field diffraction from apertures whose shape lies between a square and a circle has been experimentally studied. The main features of the observed diffraction patterns are qualitatively in accordance with previously reported computer simulations. From a topological point of view, these results no longer exhibit the square and the circle as isolated aperture cases but as a continuous deformation, which may be tackled with numerical evaluations that can be qualitatively compared with experimental observations.

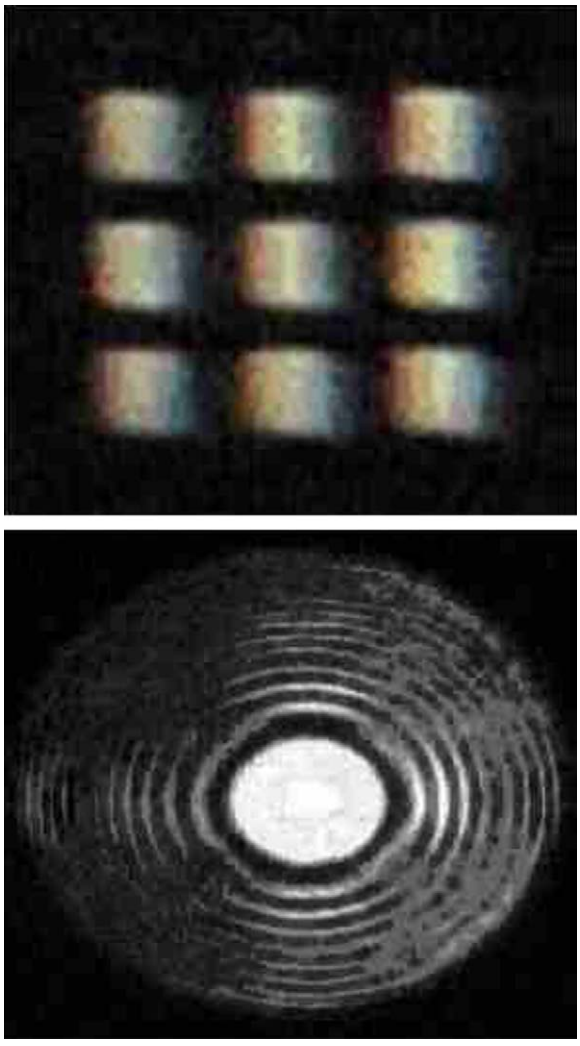

Fig. 6. Image of an LCD nine pixel array (top) and its diffraction pattern in the far field (bottom).

These types of apertures adequately describe LCD pixels that have square shapes but with slightly blunt corners. The diffraction pattern produced by an LCD single pixel has been compared with the computer-generated apertures. From this data, the pixel has been shown to have a squareness parameter close to 0.9. The features arising from the single aperture shape have been shown to remain present when an aperture array is used. The generalization of the squircle equation in order to describe figures that vary from rectangles to ellipses is straight forward [6]. Such rectangular/elliptic shapes may be more appropriate to model other digital imaging systems.

Acknowledgements

We are grateful to Prof. Caravaglia and his group for the recording of the diffraction patterns produced by the computer generated masks.

References

[1] M. Fernandez Guasti, M. De la Cruz Heredia, Diffraction pattern of a circle/square aperture, J. Mod. Opt. 40 (6) (1993) 1073–1080.
[2] W. Linnik, Simple interferomenter to test optical systems, CR Acad. Sci. URSS 1 (1933) 208
Abstract in Z. Instrum. 54 (1934) 463.
[3] W.H. Steel, Interferometry, Cambridge Studies in Modern Optics, second ed., Cambridge University Press, Cambridge, 1986.
[4] C.R. Mercer, K. Creath, Liquid-crystal point-diffraction interferometer for wave-front measurement, Appl. Opt. 35 (1996) 1633–1642.
[5] A. Meléndez Cobarrubias, Interferómetro de difracción por punto implementado en una pantalla de cristal líquido, M.Sc. Thesis, INAOE, Puebla, México, 2003.
[6] M. Fernandez Guasti, Analytic geometry of some rectilinear figures, Int. J. Educ. Sci. Technol. 23 (6) (1992) 895–901.
[7] J.W. Goodman, Introduction to Fourier Optics, McGraw Hill, San Francisco, 1968.